

SAQ-SAM: Semantically-Aligned Quantization for Segment Anything Model

Jing Zhang^{1,2}, Zhikai Li^{1,2,*}, Qingyi Gu^{1,*}

¹ Institute of Automation, Chinese Academy of Sciences

² School of Artificial Intelligence, University of Chinese Academy of Sciences

Abstract

Segment Anything Model (SAM) exhibits remarkable zero-shot segmentation capability; however, its prohibitive computational costs make edge deployment challenging. Although post-training quantization (PTQ) offers a promising compression solution, existing methods yield unsatisfactory results when applied to SAM, owing to its specialized model components and promptable workflow: (i) The mask decoder’s attention exhibits extreme outliers, and we find that aggressive clipping (ranging down to even $100\times$), instead of smoothing or isolation, is effective in suppressing outliers while maintaining semantic capabilities. Unfortunately, traditional metrics (e.g., MSE) fail to provide such large-scale clipping. (ii) Existing reconstruction methods potentially neglect prompts’ intention, resulting in distorted visual encodings during prompt interactions. To address the above issues, we propose SAQ-SAM in this paper, which boosts PTQ of SAM with semantic alignment. Specifically, we propose Perceptual-Consistency Clipping, which exploits attention focus overlap as clipping metric, to significantly suppress outliers. Furthermore, we propose Prompt-Aware Reconstruction, which incorporates visual-prompt interactions by leveraging cross-attention responses in mask decoder, thus facilitating alignment in both distribution and semantics. To ensure the interaction efficiency, we also introduce a layer-skipping strategy for visual tokens. Extensive experiments are conducted on different segmentation tasks and SAMs of various sizes, and the results show that the proposed SAQ-SAM consistently outperforms baselines. For example, when quantizing SAM-B to 4-bit, our method achieves 11.7% higher mAP than the baseline in instance segmentation task.

1. Introduction

Segment Anything Model [10] (SAM) shows promising applications as the base model for promptable segmentation. Benefiting from sufficient pre-training and prompt-guided

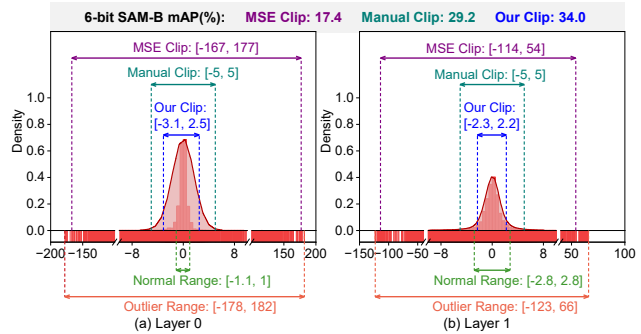


Figure 1. Visualization of extreme activation distributions and different clipping results. QK activations in the mask decoder show highly skewed distributions, with most data concentrated in a narrow range while outliers can exceed 180 times the normal range. MSE provides an overly wide clipping range, whereas our Perception-Consistency Clipping method can identify outliers more precisely. The activation tensors are hooked from the Query input in the mask decoder.

fine-tuning, SAM exhibits strong zero- or few-shot generalization capability to interactively segment regions of interest to the user. However, SAM’s powerful representation capability is accompanied by a large number of parameters and high computational costs, limiting its potential on resource-constrained devices [2, 38].

Model quantization can reduce computational overhead and model size by converting weights and activations to low-bit integers [4, 5, 7], and post-training quantization (PTQ) [11, 26], which efficiently calibrates quantization parameters using a small set of unlabeled data, stands out as a promising approach. Unfortunately, SAM features the unique activation distribution and network architecture, which pose new challenges to PTQ, rendering conventional methods inadequate. To this end, several studies have attempted to propose specific solutions for SAM’s characteristics. For instance, PQ-SAM [21] hierarchically clusters similar channels to learn unified transformation factors. However, it is limited to the image encoder with a classical Transformer structure and lacks adaptability to the mask decoder, which features more complex connection paths.

*Corresponding author: {zhikai2020, qingyi.gu}@ia.ac.cn.

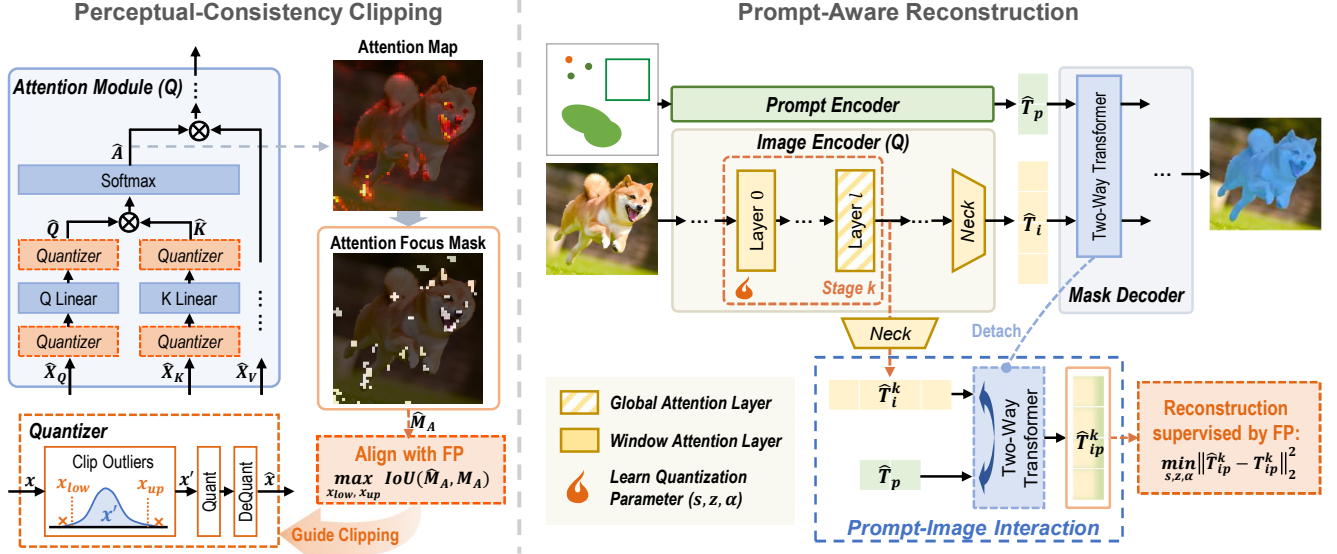


Figure 2. Overview of SAQ-SAM. The proposed Perceptual-Consistency Clipping method guides QK activation quantization clipping by minimizing the Attention Focus deviation from FP, thereby semantically preserving the perceptual alignment. Our Prompt-Aware Reconstruction method incorporates prompt-image interactions within the mask decoder into local reconstruction. Through minimizing the interaction response error supervised by the FP model, quantization model learns correspondence between visual features and prompt intentions, thus facilitating dual alignment at both the distributional and semantic levels.

In practice, although SAM’s parameters are primarily concentrated in the image encoder, the mask decoder can also introduce significant computational overhead. For example, in panoramic semantic segmentation task, given a single image, the mask decoder must perform multiple large-batch inferences for numerous prompts, whereas the image encoder only requires a single forward pass [1]. Thus, PTQ4SAM [21] proposes an improvement for quantization bottleneck in the mask decoder, which merges bimodal distributions in post-key-linear activations through QK equivalence transformation. However, the performance of these methods, which aim to better align the full-precision model (FP) at distribution level, is still far from satisfactory, especially for low-bit quantization.

In this paper, we empirically observe that the QK activation distribution of SAM’s mask decoder exhibits extreme outliers, forming a bottleneck for quantization performance. To deal with outliers, traditional methods typically employ smoothing or isolation schemes. Nevertheless, the mask decoder struggles to adapt to these methods due to its complex connection paths. Fortunately, we find an interesting phenomenon: directly clipping these outliers with an aggressive magnitude has very little impact on the final segmentation performance. For example, with SAM-B’s query input range spanning $[-178, 182]$, aggressively truncating it to $[-5, 5]$ does not hurt any accuracy. This is because, although modifying the original distribution, it maintains the semantic alignment, as shown in Figure 3. It is well-known that

quantization typically benefits from a more compact clipping range for higher resolution, for example, using the clipping range of $[-5, 5]$ yields an 11.8% mAP improvement (from 17.4% to 29.2%) for 6-bit SAM-B. However, traditional distance metrics (e.g., MSE), which aim to align distributions, fail to provide such large-scale clipping. For example, as illustrated in Figure 1, MSE gives a clipping range of $[-167, 177]$, which results in severe degradation of accuracy (from 37.0% in FP to 17.4%). Thus, instead of the distributional level, we aim to establish a semantic-level metric that facilitates effective outlier clipping by ensuring semantic alignment. Moreover, previous quantization reconstruction methods primarily focus on local reconstruction of FP responses while neglecting the semantic intent of prompts. This oversight leads to overfitting on calibration images, thus causing feature distortions in visual-prompt interactions and ultimately compromising segmentation accuracy. To this end, we are also motivated to explore the integration of prompt interactions into the reconstruction process to facilitate semantic alignment.

With the above insights, we propose SAQ-SAM, which significantly improves PTQ performance for SAM by promoting semantic-level alignment with the FP model. Specifically, we propose Perceptual-Consistency Clipping to drastically suppress outliers in QK activations, without smoothing or isolation operations. By proactively measuring the quantization-induced deviation of attention focus, the clipping range is determined without being affected by

the magnitude of outliers. As illustrated in Figure 3, our method evidently mitigates the attention functional degradation issue that is obvious in distribution-level alignment methods (e.g., MSE), thereby maintaining semantic consistency. Furthermore, we propose Prompt-Aware Reconstruction, which learns quantization parameters under the guidance of prompts. By leveraging the mask decoder to facilitate interaction between prompts and image tokens, we reconstruct the interaction responses supervised by the FP model. This preserves the correspondence between visual features and prompts, as well as alleviating the overfitting issue of local response reconstruction methods. The main contributions are summarized as follows:

- We observe that aggressively clipping outliers in SAM has minimal impact on segmentation performance. With this insight, we propose Perceptual-Consistency Clipping, which utilizes attention focus deviation as a metric to guide large-magnitude clipping, and thus suppressing outliers while maintaining semantic alignment.
- We propose Prompt-Aware Reconstruction, which integrates prompt-image interactions within the mask decoder into local reconstruction. This enables the quantized model to align with the FP model in both visual features and prompt intentions, thus facilitating dual alignment at the distributional and semantic levels.
- We conduct extensive experiments on SAMs of various sizes across both prompt segmentation and panoptic semantic segmentation tasks, demonstrating the consistent superiority of SAQ-SAM over baseline methods. For instance, in instance segmentation, our 4-bit SAQ-SAM achieves an average 14% mAP improvement on SAM-B and maintains nearly lossless accuracy on SAM-L.

2. Related Work

2.1. Segment Anything

Segment Anything [10, 27] (SAM) has emerged as a versatile and promptable image segmentation model. Trained on an extensive dataset comprising over 11 million images and 1 billion masks, SAM demonstrates remarkable generalization across various downstream applications, including edge detection, object proposal, and instance segmentation. Its capabilities extend to critical domains such as medical image annotation [3, 24], where it shows significant promise as a powerful diagnostic support tool. However, SAM’s powerful capabilities come with extensive memory and computational costs. Although some studies have proposed various lightweight variants to accelerate inference [35, 36, 39], the model parameters of these methods are still kept in floating-point type. This prevents them from benefiting from efficient low-precision integer operation units, resulting in suboptimal efficiency.

2.2. Post-Training Quantization

Model quantization [7, 14, 15] reduces memory and computation costs by converting floating-point values to integers. To mitigate performance degradation, various works were proposed, which are broadly categorized into two types: Quantization-Aware Training (QAT) and PTQ. QAT fine-tunes quantized models with labeled data at high cost [8, 13], while PTQ efficiently uses a handful of unlabeled samples to set quantization parameters [18, 25].

SAM utilizes Transformer structures for both its image encoder and mask decoder. Various works have dedicated to developing PTQ methods for Transformer structures. SmoothQuant [33] employs equivalent transformations to smooth the activation distribution, mitigating the impact of harmful outliers. OmniQuant [30] improves the applicability of smoothing methods by making equivalent transformation factors and clipping ranges learnable. RepQ-ViT [16] and RepQuant [17] decouple quantization from inference, bridging the gap through scale reparameterization for efficient hardware-friendly quantization. Besides these distribution-adjustment methods, some methods exploit the characteristics of the attention mechanism. For example, PTQ-ViT [22] determines quantization clipping by maintaining attention rank consistency and search mixed-precision scheme using the nuclear norm of module response. Other methods, such as BRECCQ [11], QDrop [32], and PD-Quant [20], aim to learn optimal quantization parameters. They reconstruct the internal response of the quantized model under the supervision of the FP model.

Despite the aforementioned methods have achieved remarkable performance in dealing with Transformer structures, SAM’s distinctive activation distribution poses new challenges, leaving their performance subpar. To this end, several works try to make improvements. To tackle the channel-wise distribution imbalance in activations, PQ-SAM [21] hierarchically clusters channels with similar distributions and learns shared transformation factors for each group, thereby reducing optimization complexity. PTQ4SAM [23] identify and integrate the bimodal distribution in post-key-linear activation of SAM’s mask decoder, while implementing an adaptive granularity quantizer for post-softmax activation to adapt to different attention module. However, these distribution-level improvements have shown unsatisfactory performance in practice.

3. Method

3.1. Preliminaries

Transformer Layers in SAM: In SAM’s image encoder, the Transformer layers employ window attention and global attention alternately [12], and the former divides the image into non-overlapping windows and computes self-attention within each window without shifting. In the mask decoder,

a lightweight Two-Way Transformer is utilized to update both the image embedding and prompt tokens via cross-attention, facilitating the information interaction between prompt and image. Specifically, the token-to-image cross-attention utilizes prompt tokens as queries and employs image tokens as keys and values, whereas the image-to-token cross-attention implements the inverse configuration to ensure comprehensive feature interaction.

Quantization Calibration: The uniform quantizer is the most commonly used and deployment-friendly quantizer, which is defined as:

$$\text{Quant} : x_q = \text{clip} \left(\left\lfloor \frac{x}{s} \right\rfloor + z, 0, 2^b - 1 \right), \quad (1)$$

$$\text{DeQuant} : \hat{x} = s(x_q - z) \approx x, \quad (2)$$

where x and x_q are the floating-point and quantized values, respectively. The dequantized value \hat{x} approximates x . $\lfloor \cdot \rfloor$ is the round-to-nearest operation. clip function truncates values outside the b-bit range. The quantization scale s and zero-point z are PTQ parameters to be searched, determined by the clipping boundaries x_{low} and x_{up} as follows:

$$s = \frac{x_{up} - x_{low}}{2^b - 1}, z = \left\lfloor -\frac{x_{low}}{s} \right\rfloor. \quad (3)$$

The process of determining clipping boundaries is crucial for improving the quantization performance in PTQ, which is also called calibration.

3.2. Perceptual-Consistency Clipping

Insight. With the observation that aggressively clipping the extreme outlier in QK activations, although significantly modifying the distribution, doesn't hurt the segmentation performance, we aim to break through the limitations of distribution alignment and turn to leverage the semantic nature of attention mechanisms for potential breakthroughs. As state in [31], in Transformers architecture, the attention mechanism captures the semantic information perceived by the model. It allocates greater focus to regions of interest, thereby reinforcing the features most relevant to the task. Building on this, we seek to leverage the potential relationships modeled by attention to preserve semantic-level consistency before and after quantization.

Attention Focus Overlap metric. Inspired by this, we define high-attention tokens as perceptual focus and maximize the overlap of the focus regions in the attention maps before and after quantization, thereby maintaining consistency in attention perception. The procedure of the metric formulation is described as follows.

Denote the input of the attention module as $X_Q \in \mathbb{R}^{N_q \times D}$, $X_K, X_V \in \mathbb{R}^{N_k \times D}$. N_q and N_k are the number of query tokens and key tokens, respectively. Note that, for simplicity, the batch and head dimensions are omitted. The attention score matrix is calculated as follows:

$$A_s = X_Q W_Q \cdot (X_K W_K)^T / \sqrt{d_h} \in \mathbb{R}^{N_q \times N_k}, \quad (4)$$



Figure 3. Comparison of attention heatmaps using different outlier clipping methods. The distribution-aligned MSE method leads to significant attention degradation, whereas our semantic-aligned PCC method maintains consistency with the FP model. The heatmaps are generated from the prompt-query cross-attention module in the first layer of the mask decoder.

where $W_Q, W_K \in \mathbb{R}^{D \times d_h}$ are weights matrix of QK linear layer, d_h is the dimension for each head. The attention scores are normalized into attention weight matrix through the Softmax function as follows:

$$A_w = \text{Softmax}(A_s) = (\alpha_1, \dots, \alpha_{N_k})^T \in \mathbb{R}^{N_q \times N_k}, \quad (5)$$

where attention weight vector $\alpha_i = (\alpha_{i,1}, \dots, \alpha_{i,N_k})^T \in \mathbb{R}^{N_k}$ represent the similarity of i-th query vector $q_i \in \mathbb{R}^{d_h}$ to all key vectors $\{k_j \in \mathbb{R}^{d_h}, j = 1, \dots, N_k\}$. A larger weight $\alpha_{i,j}$ indicates that q_i more closely matched to k_j , and the model considers the corresponding value vector v_j to be more important for the task at hand.

Given the above attention scores, we aim to distinguish salient regions and define them as the **Attention Focus**. To achieve this, threshold factor $\theta \in (0, 1)$ is used to filter the significant values, resulting in a binarized **Attention Focus Mask** as follows:

$$M_A = M(A_w) = \mathbb{1} \{A_w > \theta \cdot \max(A_w)\} \in \mathbb{R}^{N_q \times N_k}, \quad (6)$$

where $\mathbb{1} \{ \cdot \}$ represents an indicator function that returns 1 if the condition is true, otherwise 0.

The Attention Focus Mask implies critical perceptual information modeled by this attention module. On this basis, we can maintain the consistency of focusing patterns with the FP model, and thus enabling alignment at the semantic level. Specifically, we define the **Attention Focus Overlap** metric, which calculate the overlap of the Attention Focus

Mask before and after quantization as follows:

$$\text{IoU}_{\text{AF}}(A_w, \hat{A}_w) = \frac{|M_A \cap \hat{M}_A|}{|M_A \cup \hat{M}_A|}, \quad (7)$$

where the variables with a hat superscript (\hat{A}_w/\hat{M}_A) denote the scores/masks from the quantized model. This metric lies in the range (0,1), and the distance function for Perceptual-Consistency Clipping is defined as:

$$\text{Dist}_{\text{pcc}} = 1 - \text{IoU}_{\text{AF}}(A_w, \hat{A}_w). \quad (8)$$

Then, we leverage the defined Attention Focus Overlap metric to determine the optimal clipping boundaries (*i.e.* x_{low} and x_{up}) for QK activations. Unlike conventional methods constrained by distributional limitations, our proposed clipping metric operates at a semantic level, enabling more effective clipping decisions. As shown in Figure 3, while MSE-based calibration causes severe attention degradation, our clipping method achieves closer results to the FP model, efficiently preserves the perceptual capabilities of the quantized attention module.

Note that the proposed metric is specifically applied to QK activations, while other activations continue to be calibrated using the MSE metric. This strategy enables a balanced trade-off between distributional alignment and semantic fidelity across the model. By maintaining this balance, we prevent the risk of overemphasizing semantic alignment, which could otherwise lead to distributional collapse and degrade overall model performance.

3.3. Prompt-Aware Reconstruction

Insight. Quantization reconstruction methods typically learn the quantization parameters $\{s, z, \alpha\}$ by locally minimizing the error of block response under the supervision of the FP model as follows:

$$\min_{s, z, \alpha} \left\| \hat{O}^l - O^l \right\|_2^2, \quad (9)$$

where O^l, \hat{O}^l are the outputs of l -th block from the FP model and quantized model, respectively. α is the adaptive rounding factor, an extra weight quantization parameter introduced by AdaRound [26]. While this approach effectively enhances PTQ performance on conventional models, it struggles with the SAM model, particularly due to severe overfitting to pure image information. In the SAM model, to achieve the desired result, the image embedding produced by the image encoder is utilized to interact with prompt tokens in the mask decoder. However, simply considering local visual response overlooks the prompt’s intent, potentially adding redundant information that disrupts the interaction between the prompt and image features, resulting in distorted segmentation results.

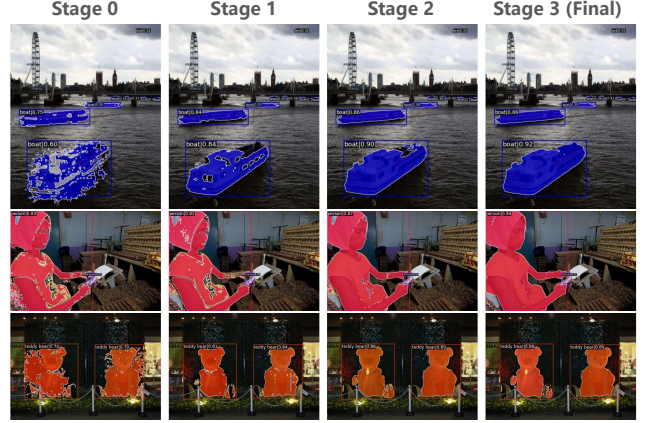


Figure 4. Segmentation results with image tokens from different stages. The output features of each stage are capable of skipping subsequent propagate while ensuring competent segmentation, with quality improving at deeper stages.

Interaction Response Reconstruction. To address the aforementioned issue, we incorporate the interaction between prompt and image tokens into the reconstruction process, enabling more effective matching under the supervision of the FP model. Specifically, instead of aligning the local visual response, we reconstruct the hybrid image tokens that incorporate the prompt information by leveraging the interaction in the mask decoder.

As illustrated in Figure 2, we utilize the off-the-shelf interaction module in SAM’s mask decoder to incorporate prompt information for the image tokens, without additional components or extra training. In this way, the hybrid image tokens can be obtained as follows:

$$T_{ip}^k = \text{MaskDecoderModule}(T_i^k, T_p), \quad (10)$$

where T_p denotes prompt tokens encoded by prompt encoder, T_i^k denotes image tokens derived from the output of the k -th stage. MaskDecoderModule refers to Two-Way Transformer, which is the primary interaction module in the mask decoder. Subsequently, these tokens are reconstructed to learn the quantization parameters, *i.e.*, minimizing the L2 distance between the hybrid image tokens and the corresponding response in the FP model as follows:

$$\min_{s, z, \alpha} \left\| \hat{T}_{ip}^k - T_{ip}^k \right\|_2^2, \quad (11)$$

where T_{ip}^k and \hat{T}_{ip}^k are tokens from the FP model and the quantized model, respectively.

Note that to ensure efficiency of the prompt-image interactions, the defined image tokens T_i^k skip subsequent layers and directly perform dimensionality reduction through the neck. This approach avoids prohibitively high computational cost associated with complete forward passes and

gradient backpropagation, and thus only introduces a slight additional overhead compared to traditional local response reconstruction. Moreover, in addition to improving efficiency, the layer-skipping strategy also offers advantages in performance retention. By shortening optimization paths, it better preserves local distributional properties and reduces the loss of interaction information that may occur due to excessively long propagation processes.

To validate the effectiveness of utilizing these skip-layer tokens for interaction, we conduct verification experiments in which these tokens are used as the final visual embeddings to participate in the mask decoder inference. The segmentation results, as shown in Figure 4, demonstrate that the outputs from each stage are capable of producing rational segmentation results without further processing by subsequent layers. This provides implicit evidence that the proposed approach enables an effective interaction, with the outputs of each stage functioning as image embeddings at different levels of granularity.

To further enhance the efficiency of parameter learning and improve overall performance, we partition the Transformer layers into multiple stages and adopt a stage-wise learning approach for quantization parameters, where the parameters within each stage are jointly optimized. Previous work [29] has demonstrated the superiority of jointly optimizing multiple quantization blocks in reconstruction, as it effectively captures weight correlations across blocks. Building on this insight, we intuitively define global attention layers as boundaries for stage partitioning. For example, in SAM-B, layers L_2, L_5, L_8 and L_{11} employ global attention, while the remaining layers utilize window attention. Accordingly, layers $\{L_0, L_1, L_2\}$ constitute stage 0, and this pattern repeats for subsequent stages.

4. Experiment

4.1. Experimental Setup

Tasks and Datasets. Our experiments focus on two prevalent SAM practices: instance segmentation and semantic segmentation. In instance segmentation tasks, SAM generates segmentation masks according to provided bounding boxes. The manual prompting process is substituted by a detector that identifies the target objects within the image and produces the corresponding bounding boxes’ coordinates for SAM. We evaluate the performance of the quantized SAM on the MS-COCO [19] dataset, with the mean Average Precision (mAP) serving as evaluation metric. In the semantic segmentation experiment, SAM is employed to enhance the quality of segmentation masks produced by traditional semantic segmentor. A large number of points, which are evenly distributed across the image, act as prompts. These prompts are fed into SAM in multiple batches, generating a plenty of masks. Through a se-

ries of post-processing steps, these masks are matched with the outputs of semantic segmentor, thus forming the final panoptic segmentation result [1]. The evaluation dataset is ADE20K [40], with mean Intersection over Union (mIoU) serving as performance metric.

Implementation Details. We take PTQ4SAM [23] as the baseline method, while maintaining largely consistent experimental settings for fair comparison. To be specific, the quantization scheme employs per-tensor asymmetric quantization for activations and per-channel asymmetric quantization for weights, with exceptions for the first and last layers which remain unquantized. The calibration set contains 32 images randomly sampled from the training dataset. For the Perception-Consistency Clipping (PCC) method, we set threshold factor θ to 0.5. All QK activations (i.e., the inputs and outputs of Query Linear and Key Linear) are calibrated based on Attention Focus Overlap metric using the first sample, while other activations are calibrated based on Mean Squared Error (MSE) using all samples. The weights are calibrated using the MSE. For Prompt-Aware Reconstruction (PAR), the image encoder employs stage-wise learning, while the mask decoder employs layer-wise learning with 2000 iterations. Exceptionally, the additional cross-attention block that is equipped at the end of the mask decoder learns 10000 iterations due to its large loss. In general, compared to PTQ4SAM settings, which carry block-wise learning with 20000 iterations, our method requires much lower time cost.

Baseline Methods. We use the advanced PTQ4SAM as our baseline [23]. For comparative analysis, we categorize the methods into two groups according to whether there is a learning process or not. For the first group of statistic-based PTQ methods, we integrated the PCC method into PTQ4SAM-S [23], and this is referred to as SAQ-PCC. As for the second group of learning-based PTQ methods, we build on PTQ4SAM-L [23] and substitute the QDrop [32] with our PAR method, which is abbreviated as SAQ-PAR. When the PCC method is further incorporated as a pre-processing step, our complete method, denoted as SAQ-SAM, is established.

4.2. Instance Segmentation Results

In the task of instance segmentation, we provide a detailed comparison of the performance on various sizes of SAM, including SAM-B, SAM-L and SAM-H, when used in conjunction with different detectors (including Faster R-CNN [28], YOLOX [6], H-Deformable-DETR [9], and DINO [37]). The results on COCO dataset are listed in Table 1. Our method consistently shows superior performance. Compared to baseline PTQ4SAM-S [23], SAQ-PCC achieves a nearly twofold improvement in mAP for 6-bit SAM-B (e.g., from 20.4% to 39.4% with DINO) and recovers the collapsed accuracy to an average of 2.7% mAP at

Table 1. Quantization results of instance segmentation on COCO datasets with various detectors as prompt providers. Here, we abbreviate ‘Reconstruction’ as ‘REC’, ‘ $WxAy$ ’ denotes the weights and activations are quantized to x bit and y bit, respectively, and ‘-’ indicates the mAP is below 1. The bolded values represent the best-performing results under the same settings.

Detector	Methods	REC	SAM-B			SAM-L			SAM-H		
			FP	W6A6	W4A4	FP	W6A6	W4A4	FP	W6A6	W4A4
Faster R-CNN [28]	PTQ4SAM-S [23]	✗	33.4	15.4	-	36.4	35.7	18.1	37.2	36.0	24.1
	SAQ-PCC	✗		29.8	2.8		35.7	20.9		36.1	25
	PTQ4SAM-L [23]	✓		30.3	16.0		35.8	28.7		36.5	33.5
	SAQ-PAR	✓		31.9	23.2		35.8	34.6		36.7	35.9
	SAQ-SAM (PCC+PAR)	✓		32.0	27.7		35.9	34.5		36.6	35.9
YOLOX [6]	PTQ4SAM-S [23]	✗	37.0	17.4	-	40.4	40.0	20.6	41.0	40.3	26.7
	SAQ-PCC	✗		34.0	2.1		40.0	24.2		40.2	28.4
	PTQ4SAM-L [23]	✓		34.3	18.4		40.3	31.6		40.7	37.6
	SAQ-PAR	✓		35.7	26.2		40.2	38.9		40.8	39.4
	SAQ-SAM (PCC+PAR)	✓		35.9	30.3		40.3	39.0		40.9	39.9
H-Deformable-DETR [9]	PTQ4SAM-S [23]	✗	38.2	17.9	-	41.5	41.0	20.9	42.0	41.3	27.3
	SAQ-PCC	✗		36.4	2.6		41.1	24.3		41.3	28.2
	PTQ4SAM-L [23]	✓		35.1	17.3		41.2	32.1		41.6	38.4
	SAQ-PAR	✓		37.0	29.4		41.2	39.6		41.9	40.8
	SAQ-SAM (PCC+PAR)	✓		37.1	31.8		41.3	39.8		41.8	40.7
DINO [37]	PTQ4SAM-S [23]	✗	44.5	20.4	-	48.6	47.7	23.1	49.1	48.1	30.5
	SAQ-PCC	✗		39.4	3.5		48.0	27.8		48.2	31.6
	PTQ4SAM-L [23]	✓		40.4	14.4		48.3	36.6		48.7	43.9
	SAQ-PAR	✓		42.3	30.2		48.3	46.1		48.8	47.4
	SAQ-SAM (PCC+PAR)	✓		42.4	33.8		48.3	46.3		48.9	47.4

4-bit. For SAM-L and SAM-H, the advantages are particularly evident in low-bit settings. For example, SAQ-PCC increases the mAP of 4-bit SAM-L from 23.1% to 27.8% with DINO, and increases the mAP of 4-bit SAM-H from 26.7% to 28.4% with YOLOX. In terms of reconstruction methods, compared to PTQ4SAM-L [23] that uses naive QDrop, our methods achieve significant improvement with lower computational costs. For example, SAQ-PAR improves the 6-bit SAM-B by 1.6% mAP (from 30.3% to 31.9%), and the 4-bit SAM-B by 7.2% (from 16.0% to 23.2%), both with Faster R-CNN. For larger models, it boosts 4-bit SAM-L by 9.5% (from 36.6% to 46.1%) with DINO. Furthermore, if used as a pre-processing step, PCC can provide more favorable initial values for PAR optimization, thereby further enhancing the performance of low-bit quantization. For example, SAQ-SAM improves the 4-bit SAM-B by 14.5% mAP (from 17.3% to 31.8% with H-Deformable-DETR) and achieves near-lossless accuracy for 4-bit SAM-L and SAM-H (e.g., with only a drop of 1.4% for SAM-L with YOLOX, and 1.3% for SAM-H with Faster R-CNN).

Table 2. Quantization results of semantic segmentation on ADE20K datasets with SegFormer providing category labels.

Model	Prec.	Method	REC	mIoU(%)
	FP	-	-	33.17
SAM-B	W6A6	PTQ4SAM-S [23]	✗	31.16
	W6A6	SAQ-PCC	✗	32.90
	W6A6	PTQ4SAM-L [23]	✓	32.65
	W6A6	SAQ-SAM	✓	33.04
	W4A4	PTQ4SAM-S [23]	✗	31.08
	W4A4	SAQ-PCC	✗	31.29
	W4A4	PTQ4SAM-L [23]	✓	31.85
	W4A4	SAQ-SAM	✓	32.53

4.3. Semantic Segmentation Results

In the task of semantic segmentation, we employed SegFormer [34] as the semantic branch, which provides cat-

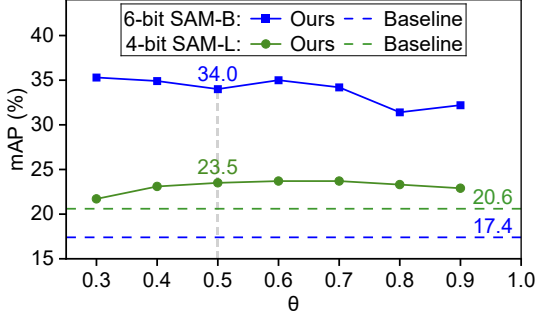


Figure 5. Curve plots of ablation experiment results for attention focus threshold θ . The performance of our method is robust to this hyperparameter, and the result consistently outperform the baseline, with 0.5 being a modest choice.

egory labels for SAM’s masks. The test results on the ADE20K dataset are reported in Table 2. Since the masks generated by SAM are exposed to a series of post-processing procedures, the harm caused by quantization on the final performance is not as obvious. Nevertheless, our methods improve the accuracy of quantized SAM-B comprehensively. For example, SAQ-PCC increases the accuracy of 6-bit quantization by 1.74% mIoU (from 31.16% to 32.9%), even surpassing the learning-based PTQ4SAM-L (with 32.65% mIoU). Furthermore, SAQ-SAM boosts the performance close to FP, with only a loss of 0.13% mIoU at 6 bits and a loss of 0.64% at 4-bit.

4.4. Ablation Study

4.4.1. Attention Focusing Threshold Setting

In the proposed PCC module, we use the threshold factor θ to define the focus area of attention. For generality, we typically set θ to 0.5. To explore the impact of this hyperparameter on the performance of our method, we carry out comparative experiments on the instance segmentation task. Setting θ to values ranging from 0.3 to 0.9, the results on 6-bit SAM-B and 4-bit SAM-L are shown in Figure 5. Our analysis indicates two key points: First, with changes in θ , the performance of our clipping method slightly fluctuates, but it consistently outperforms the baseline method, with 0.5 emerging as a modest choice. Second, our method demonstrates exceptional robustness to the setting of θ , achieving satisfactory performance across a range of values from 0.4 to 0.7.

4.4.2. Comparison of Reconstruction Method

Inspired by [29], we partition several layers into a *stage* based on the global attention layer, and treat these *stages* as optimization units. This scheme not only reduces the computation cost, but also captures the dependencies among blocks, which achieves superior performance. To investigate the effectiveness of our PAR method under differ-

Table 3. Ablation study for reconstruction methods using different optimization unit partitions. The per-stage reconstruction exhibits a greater superiority and our method outperforms the baseline at both reconstruction granularities

Prec.	Method	Per-Layer	Per-Stage
W4A4	QDrop	8.1	17.9
	PAR	24.4	26.2
	QDrop+PCC	16.5	26.6
	PAR+PCC	28.6	30.3
W6A6	QDrop	33.7	35.6
	PAR	35.7	35.7
	QDrop+PCC	34.4	35.8
	PAR+PCC	35.8	35.9

ent reconstruction granularities (per-layer and per-stage), we conduct detailed ablation experiments, comparing the performance of using QDrop reconstruction, our Prompt-Aware Reconstruction, and the cases where PCC is used as prior processing. We quantized SAM-B for instance segmentation with YOLOX as the detector. The experimental results are shown in the Table 3. Note that, for fair comparison, the learning settings across all experiments are kept consistent, including learning iterations, learning rate, optimizer and drop probability. The results show that compared with per-layer learning, consistently exhibits advantages across various methods, indicating that the per-stage granularity is a more effective choice. Furthermore, our method demonstrates superior performance under both reconstruction granularities, highlighting the contribution of introducing interactions into the reconstruction process.

5. Conclusion

In this paper, we propose SAQ-SAM, a post-training quantization framework for the SAM model. To address the issue of extreme outliers in mask decoder’s QK activations, we introduce a semantically-preserved outlier clipping approach, which can effectively suppress significant outliers without smoothing or isolation. Specifically, we determine the optimal clipping boundary by minimizing the attention focus deviation caused by quantization, overcoming the limitations of distribution-based methods. Furthermore, we incorporate prompt-image interactions into reconstruction, which learns the correlation between visual features and prompt intent, thereby achieving alignment at both semantic and distributional levels. To improve the interaction efficiency, we also introduce a layer-skipping strategy and a stage-partitioning approach. Extensive experiments show that our method significantly outperforms baseline methods, especially in low-bit scenarios. In the future, one could extend this approach to accelerate SAM2, which is a promising method for video segmentation acceleration.

References

- [1] Jiaqi Chen, Zeyu Yang, and Li Zhang. Semantic segment anything. <https://github.com/fudan-zvg/Semantic-Segment-Anything>, 2023. 2, 6
- [2] Zigeng Chen, Gongfan Fang, Xinyin Ma, and Xinchao Wang. Slimsam: 0.1% data makes segment anything slim. *arXiv preprint arXiv:2312.05284*, 2023. 1
- [3] Junlong Cheng, Jin Ye, Zhongying Deng, Jianpin Chen, Tianbin Li, Haoyu Wang, Yanzhou Su, Ziyang Huang, Jilong Chen, Lei Jiang, et al. Sam-med2d. *arXiv preprint arXiv:2308.16184*, 2023. 3
- [4] Jungwook Choi, Zhuo Wang, Swagath Venkataramani, Pierce I-Jen Chuang, Vijayalakshmi Srinivasan, and Kailash Gopalakrishnan. Pact: Parameterized clipping activation for quantized neural networks. *arXiv preprint arXiv:1805.06085*, 2018. 1
- [5] Steven K Esser, Jeffrey L McKinstry, Deepika Bablani, Rathinakumar Appuswamy, and Dharmendra S Modha. Learned step size quantization. In *International Conference on Learning Representations*, 2020. 1
- [6] Zheng Ge, Songtao Liu, Feng Wang, Zeming Li, and Jian Sun. Yolox: Exceeding yolo series in 2021. *arXiv preprint arXiv:2107.08430*, 2021. 6, 7
- [7] Amir Gholami, Sehoon Kim, Zhen Dong, Zhewei Yao, Michael W Mahoney, and Kurt Keutzer. A survey of quantization methods for efficient neural network inference. *arXiv preprint arXiv:2103.13630*, 2021. 1, 3
- [8] Benoit Jacob, Skirmantas Kligys, Bo Chen, Menglong Zhu, Matthew Tang, Andrew Howard, Hartwig Adam, and Dmitry Kalenichenko. Quantization and training of neural networks for efficient integer-arithmetic-only inference. In *Proceedings of the IEEE conference on computer vision and pattern recognition*, pages 2704–2713, 2018. 3
- [9] Ding Jia, Yuhui Yuan, Haodi He, Xiaopei Wu, Haojun Yu, Weihong Lin, Lei Sun, Chao Zhang, and Han Hu. Detsr with hybrid matching. In *Proceedings of the IEEE/CVF conference on computer vision and pattern recognition*, pages 19702–19712, 2023. 6, 7
- [10] Alexander Kirillov, Eric Mintun, Nikhila Ravi, Hanzi Mao, Chloe Rolland, Laura Gustafson, Tete Xiao, Spencer Whitehead, Alexander C Berg, Wan-Yen Lo, et al. Segment anything. In *Proceedings of the IEEE/CVF international conference on computer vision*, pages 4015–4026, 2023. 1, 3
- [11] Yuhang Li, Ruihao Gong, Xu Tan, Yang Yang, Peng Hu, Qi Zhang, Fengwei Yu, Wei Wang, and Shi Gu. Brecq: Pushing the limit of post-training quantization by block reconstruction. *arXiv preprint arXiv:2102.05426*, 2021. 1, 3
- [12] Yanghao Li, Hanzi Mao, Ross Girshick, and Kaiming He. Exploring plain vision transformer backbones for object detection. In *European conference on computer vision*, pages 280–296. Springer, 2022. 3
- [13] Zhikai Li and Qingyi Gu. I-vit: Integer-only quantization for efficient vision transformer inference. In *Proceedings of the IEEE/CVF International Conference on Computer Vision*, pages 17065–17075, 2023. 3
- [14] Zhikai Li, Liping Ma, Mengjuan Chen, Junrui Xiao, and Qingyi Gu. Patch similarity aware data-free quantization for vision transformers. In *European Conference on Computer Vision*, pages 154–170. Springer, 2022. 3
- [15] Zhikai Li, Xiaoxuan Liu, Banghua Zhu, Zhen Dong, Qingyi Gu, and Kurt Keutzer. Qft: Quantized full-parameter tuning of llms with affordable resources. *arXiv preprint arXiv:2310.07147*, 2023. 3
- [16] Zhikai Li, Junrui Xiao, Lianwei Yang, and Qingyi Gu. Repqvit: Scale reparameterization for post-training quantization of vision transformers. In *Proceedings of the IEEE/CVF International Conference on Computer Vision*, pages 17227–17236, 2023. 3
- [17] Zhikai Li, Xuewen Liu, Jing Zhang, and Qingyi Gu. Repquant: Towards accurate post-training quantization of large transformer models via scale reparameterization. *arXiv preprint arXiv:2402.05628*, 2024. 3
- [18] Ji Lin, Jiaming Tang, Haotian Tang, Shang Yang, Wei-Ming Chen, Wei-Chen Wang, Guangxuan Xiao, Xingyu Dang, Chuang Gan, and Song Han. Awq: Activation-aware weight quantization for on-device llm compression and acceleration. *Proceedings of Machine Learning and Systems*, 6:87–100, 2024. 3
- [19] Tsung-Yi Lin, Michael Maire, Serge Belongie, James Hays, Pietro Perona, Deva Ramanan, Piotr Dollár, and C Lawrence Zitnick. Microsoft coco: Common objects in context. In *Computer vision—ECCV 2014: 13th European conference, Zurich, Switzerland, September 6–12, 2014, proceedings, part v 13*, pages 740–755. Springer, 2014. 6
- [20] Jiawei Liu, Lin Niu, Zhihang Yuan, Dawei Yang, Xinggang Wang, and Wenyu Liu. Pd-quant: Post-training quantization based on prediction difference metric. In *Proceedings of the IEEE/CVF Conference on Computer Vision and Pattern Recognition*, pages 24427–24437, 2023. 3
- [21] Xiaoyu Liu, Xin Ding, Lei Yu, Yuanyuan Xi, Wei Li, Zhi-jun Tu, Jie Hu, Hanting Chen, Baoqun Yin, and Zhiwei Xiong. Pq-sam: Post-training quantization for segment anything model. In *European Conference on Computer Vision*, pages 420–437. Springer, 2024. 1, 2, 3
- [22] Zhenhua Liu, Yunhe Wang, Kai Han, Wei Zhang, Siwei Ma, and Wen Gao. Post-training quantization for vision transformer. *Advances in Neural Information Processing Systems*, 34:28092–28103, 2021. 3
- [23] Chengtao Lv, Hong Chen, Jinyang Guo, Yifu Ding, and Xi-anglong Liu. Ptq4sam: Post-training quantization for segment anything. In *Proceedings of the IEEE/CVF Conference on Computer Vision and Pattern Recognition*, pages 15941–15951, 2024. 3, 6, 7
- [24] Jun Ma, Yuting He, Feifei Li, Lin Han, Chenyu You, and Bo Wang. Segment anything in medical images. *Nature Communications*, 15(1):654, 2024. 3
- [25] Markus Nagel, Mart van Baalen, Tijmen Blankevoort, and Max Welling. Data-free quantization through weight equalization and bias correction. In *Proceedings of the IEEE/CVF international conference on computer vision*, pages 1325–1334, 2019. 3
- [26] Markus Nagel, Rana Ali Amjad, Mart Van Baalen, Christos Louizos, and Tijmen Blankevoort. Up or down? adaptive rounding for post-training quantization. In *International*

- conference on machine learning*, pages 7197–7206. PMLR, 2020. 1, 5
- [27] Nikhila Ravi, Valentin Gabeur, Yuan-Ting Hu, Ronghang Hu, Chaitanya Ryali, Tengyu Ma, Haitham Khedr, Roman Rädle, Chloe Rolland, Laura Gustafson, et al. Sam 2: Segment anything in images and videos. *arXiv preprint arXiv:2408.00714*, 2024. 3
- [28] Shaoqing Ren, Kaiming He, Ross Girshick, and Jian Sun. Faster r-cnn: Towards real-time object detection with region proposal networks. *Advances in neural information processing systems*, 28, 2015. 6, 7
- [29] Khasmamad Shabanovi, Lukas Wiest, Vladimir Golkov, Daniel Cremers, and Thomas Pfeil. Interactions across blocks in post-training quantization of large language models. *arXiv preprint arXiv:2411.03934*, 2024. 6, 8
- [30] Wenqi Shao, Mengzhao Chen, Zhaoyang Zhang, Peng Xu, Lirui Zhao, Zhiqian Li, Kaipeng Zhang, Peng Gao, Yu Qiao, and Ping Luo. Omniquant: Omnidirectionally calibrated quantization for large language models. *arXiv preprint arXiv:2308.13137*, 2023. 3
- [31] Ashish Vaswani, Noam Shazeer, Niki Parmar, Jakob Uszkoreit, Llion Jones, Aidan N Gomez, Łukasz Kaiser, and Illia Polosukhin. Attention is all you need. *Advances in neural information processing systems*, 30, 2017. 4
- [32] Xiuying Wei, Ruihao Gong, Yuhang Li, Xianglong Liu, and Fengwei Yu. Qdrop: Randomly dropping quantization for extremely low-bit post-training quantization. *arXiv preprint arXiv:2203.05740*, 2022. 3, 6
- [33] Guangxuan Xiao, Ji Lin, Mickael Seznec, Hao Wu, Julien Demouth, and Song Han. Smoothquant: Accurate and efficient post-training quantization for large language models. In *International Conference on Machine Learning*, pages 38087–38099. PMLR, 2023. 3
- [34] Enze Xie, Wenhai Wang, Zhiding Yu, Anima Anandkumar, Jose M Alvarez, and Ping Luo. Segformer: Simple and efficient design for semantic segmentation with transformers. *Advances in neural information processing systems*, 34: 12077–12090, 2021. 7
- [35] Yunyang Xiong, Bala Varadarajan, Lemeng Wu, Xiaoyu Xiang, Fanyi Xiao, Chenchen Zhu, Xiaoliang Dai, Dilin Wang, Fei Sun, Forrest Iandola, et al. Efficientsam: Leveraged masked image pretraining for efficient segment anything. In *Proceedings of the IEEE/CVF Conference on Computer Vision and Pattern Recognition*, pages 16111–16121, 2024. 3
- [36] Chaoning Zhang, Dongshen Han, Yu Qiao, Jung Uk Kim, Sung-Ho Bae, Seungkyu Lee, and Choong Seon Hong. Faster segment anything: Towards lightweight sam for mobile applications. *arXiv preprint arXiv:2306.14289*, 2023. 3
- [37] Hao Zhang, Feng Li, Shilong Liu, Lei Zhang, Hang Su, Jun Zhu, Lionel M Ni, and Heung-Yeung Shum. Dino: Detr with improved denoising anchor boxes for end-to-end object detection. *arXiv preprint arXiv:2203.03605*, 2022. 6, 7
- [38] Zhuoyang Zhang, Han Cai, and Song Han. Efficientvit-sam: Accelerated segment anything model without performance loss. In *Proceedings of the IEEE/CVF Conference on Computer Vision and Pattern Recognition*, pages 7859–7863, 2024. 1
- [39] Xu Zhao, Wenchao Ding, Yongqi An, Yinglong Du, Tao Yu, Min Li, Ming Tang, and Jinqiao Wang. Fast segment anything. *arXiv preprint arXiv:2306.12156*, 2023. 3
- [40] Bolei Zhou, Hang Zhao, Xavier Puig, Sanja Fidler, Adela Barriuso, and Antonio Torralba. Scene parsing through ade20k dataset. In *Proceedings of the IEEE conference on computer vision and pattern recognition*, pages 633–641, 2017. 6